Energy and charge transfer in ionized argon coated water clusters

J. Koišek, J. Lengyel, M. Fárník, and P. Slavíek

Energy and charge transfer in ionized argon coated water clusters

J. Kočišek,[1,a)] J. Lengyel,[1,b)] M. Fárník,[1,a)] and P. Slavíček[2,a),c)]

[1]*J. Heyrovský Institute of Physical Chemistry v.v.i., Academy of Sciences of the Czech Republic, Dolejškova 3, 18223 Prague, Czech Republic*

[2]*Department of Physical Chemistry, Institute of Chemical Technology, Technická 5, 16628 Prague 6, Czech Republic*

We investigate the electron ionization of clusters generated in mixed Ar-water expansions. The electron energy dependent ion yields reveal the neutral cluster composition and structure: water clusters fully covered with the Ar solvation shell are formed under certain expansion conditions. The argon atoms shield the embedded $(H_2O)_n$ clusters resulting in the ionization threshold above ≈ 15 eV for all fragments. The argon atoms also mediate more complex reactions in the clusters: e.g., the charge transfer between Ar^+ and water occurs above the threshold; at higher electron energies above ~ 28 eV, an excitonic transfer process between Ar^{+*} and water opens leading to new products Ar_nH^+ and $(H_2O)_nH^+$. On the other hand, the excitonic transfer from the neutral Ar^* state at lower energies is not observed although this resonant process was demonstrated previously in a photoionization experiment. Doubly charged fragments $(H_2O)_nH_2^{2+}$ and $(H_2O)_n^{2+}$ ions are observed and Intermolecular Coulomb decay (ICD) processes are invoked to explain their thresholds. The Coulomb explosion of the doubly charged cluster formed within the ICD process is prevented by the stabilization effect of the argon solvent. © *2013 AIP Publishing LLC*. [http://dx.doi.org/10.1063/1.4834715]

I. INTRODUCTION

Ionization of liquid water and subsequent dynamical processes belong to the basic processes of radiation chemistry.[1,2] Isolated water molecule ionizes at 12.6 eV upon the ejection of the $1b_1$ (HOMO) electron. The ionization threshold lowers upon complexation,[3–5] being shifted by ≈ 2 eV in liquid water.[6] It is generally accepted that upon the ionization of the water HOMO orbital, a proton is transferred into a neighbouring water unit, forming hydronium cation and OH radical

$$H_2O^+ + H_2O \rightarrow H_3O^+ + OH \quad (1)$$
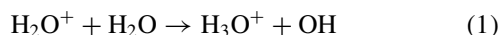
with the estimated lifetime of the H_2O^+ radical to be less than 40 fs.[7] The process (1) has almost 100% efficiency and the energy released during this process amounts to about 1 eV,[8] well above the binding energy of the OH radical to the hydronium cation. As a result, the threshold photoionization of water clusters leads almost exclusively to a formation of the $H^+(H_2O)_n$ fragments. These products are formed independently of the ionization method, i.e., both upon the photoionization and electron ionization.[9]

The ionization reaction can be realized in the "inert solvent," e.g., the experiment can be performed in mixed water-argon clusters. Under these conditions, even the non-protonated cations $(H_2O)_n^+$ are observed. Recently, the infrared spectrum of the size-selected water clusters have been recorded using the argon tagging experiment, showing that the non-protonated clusters have a structure $H_3O^+\cdots OH$, that means that the proton transfer still takes place.[10,11] The excess energy formed within the reaction (1) is taken away by the evaporation of the inert solvent atoms.[12] Similarly, the non-protonated clusters of water and more complex systems have been observed in electron impact studies including argon[13–15] and helium solvents.[16,17]

Golan and Ahmed[18] have recently pointed out that the role of the argon atoms in the photoionization of water clusters is more significant than just acting as a thermal bath. According to their study of mixed argon/water clusters exposed to a tunable VUV radiation, the ionization starts with the argon excitation. The energy is then transferred from the argon atom into the water cluster, which is ionized. The excess energy is removed from the system by previously mentioned solvent evaporation. The mediator role of argon atom in the ionization process is in many aspects remarkable. The reaction between the excited argon atom and water cluster can be viewed as the Penning ionization in the condensed phase.[19,20] Alternatively, it bears some resemblance with the recently identified Intermolecular Coulomb Decay (ICD), where the energy released in the de-excitation of one molecular unit is used to ionize a neighbouring water unit.[21,22] As the energy transfer processes in the condensed phase are so far understood rather incompletely, the mixed argon-water system appears to be a good case for a detailed study.

The electron ionization used in this work is in several respects different from the photoionization. First, the cross section for $e^- + Ar$ scattering is higher than the photoabsorption cross section at similar energies and it can be expected that only the surface argon atoms are excited/ionized by electrons. Second, the nature of the electron interaction is

a)Authors to whom correspondence should be addressed. Electronic addresses: kocisek@jh-inst.cas.cz, michal.farnik@jh-inst.cas.cz, and petr.slavicek@vscht.cz

b)Also at Department of Physical Chemistry, Institute of Chemical Technology, Technická 5, Prague 6, Czech Republic.

c)Also at J. Heyrovský Institute of Physical Chemistry v.v.i., Academy of Sciences of the Czech Republic, Dolejškova 3, 18223 Prague, Czech Republic.

139, 214308-1

different, which results into population of excited states forbidden for photonic transitions or energy shifts due to incoming-outgoing electron interaction. The relatively large energy range of the electron beam in our study allows to investigate processes going beyond the excitation/ionization of the valence electrons. The ejection of lower-lying electrons opens new reaction pathways in the ionized water clusters as was demonstrated, e.g., in our recent *ab initio* simulations.[8]

Below we present our observation on the argon mediated electron ionization of the water clusters which also revealed the structure of argon-water clusters. We further address the following questions: (1) Is the exciton transfer ionization observed upon the electron excitation of argon clusters? (2) What are the products of the ionization mediated by the ionized argon atoms? (3) Do the ICD-type processes enhance the ion formation at higher electron energies?

II. EXPERIMENT

The experiments were conducted on the CLUB (CLUster Beam) apparatus described in detail elsewhere,[23] which has recently been extended with a new reflectron time-of-flight mass spectrometer (RTOF).[24–26] The clusters were produced in an expansion of mixture of deionized water and Ar (Messer 4.5) into vacuum. The resulting molecular beam was skimmed ∼25 mm downstream the nozzle and passed ∼90 cm flight path through two differentially pumped chambers into the detection chamber hosting the RTOF. The RTOF mounted orthogonally to the molecular beam was custom built on the basis of our specifications.[26] The spectrometer provides the option to also measure the energy dependence of the mass spectra in the range 5–90 eV. The electron energy resolution was ≈0.7 eV FWHM. The energy dependent ion yields near threshold were fitted by a power function to obtain the value of appearance energy for particular ions. We used the procedure of Matejčik[27] to increase the precision of the obtained values.

In our study, we have exploited a variety of expansion conditions corresponding to different clustering regimes which are summarized in Table I. Here, we focus mainly on the clusters formed in the expansion conditions no. 7 close to that in the photoionization study in Ref. 18. The clusters generated under these conditions have the structure of Ar coated water clusters as we argue below.

The structure, composition, and size of the mixed clusters generated in the supersonic expansions cannot be determined unambiguously from the mass spectrometric experiments. However, mean cluster size estimates based on semi-empirical formulas can be made for pure expansions. The mean cluster size of Ar_n and $(H_2O)_n$ clusters can be obtained using the Hagena's scaling laws[28–31]

$$\bar{n} = K \cdot \left(\frac{\Gamma^*}{1000}\right)^\zeta, \quad \Gamma^* = \frac{p_0[\text{mbar}] \cdot d_e[\mu\text{m}]^{0.85}}{T_0[\text{K}]^{2.2875}} \cdot A, \tag{2}$$

where $A = 1646$ for Ar, and $K = 38.4$ and $\zeta = 1.64$ were determined from diffractive He atom scattering on large Ar_n clusters.[31] The equivalent nozzle diameter $d_e = k \times \frac{d}{\tan(\alpha/2)}$ is given by the nozzle throat diameter d and its opening angle α ($\alpha = 30°$, and $k = 0.736$ for Ar).

For the pure water vapour expansions, similar relations have been derived from sodium pickup experiments in the Buck's group using our present water cluster source[32]

$$\Gamma^* = \frac{n_0 \cdot d_e^q \cdot T_0^{q-3}}{K_{ch}}, \tag{3}$$

where the characteristic constant $K_{ch} = r_{ch}^{q-3} T_{ch}^{q-3}$ for H_2O derives from the molecular parameters $r_{ch} = 3.19$ Å, and $T_{ch} = 5684$ K. The stagnation pressure p_0 and gas density n_0 can be connected through ideal gas law. The parameters $K = 11.6$, $\zeta = 1.886$ (Eq. (2)) and $q = 0.634$ (and $k = 0.933$ for d_e for H_2O) were determined from fitting the measured size distributions of large $(H_2O)_n$ clusters.[32]

The mean cluster sizes calculated according to the above equations are summarized in Table I for the present expansion conditions. For pure water expansions no. 1 and 2 Eq. (3) is used, while for mixed expansions with more than 98% of Ar-content we report the mean Ar_n cluster sizes which would be generated in pure Ar expansions according to Eq. (2). For He expansions, no sizes are reported; pure He does not cluster under these conditions, yet large $(H_2O)_n$ clusters were generated in these expansions judging by the $(H_2O)H_k^+$ ionic fragments.

It ought to be stressed that the semi-empirical rules have been proved experimentally for expansions of pure gasses only, and admixture of even a small percentage of another gas can change the conditions significantly. By the way of example, pure $(HBr)_n$ clusters were predominantly generated when even less than 5% of HBr was added in Ar expansion

TABLE I. The expansion conditions exploited in present work. The mean neutral cluster sizes $\bar{n}$ correspond to estimates made for pure H_2O or Ar expansions as outlined in the text. Note that the mixed expansions are further discussed in the text.

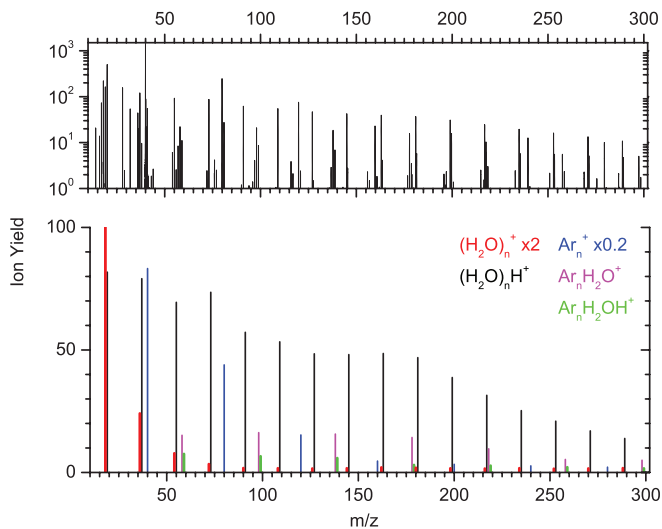| No.:	Gas	Reservoir/nozzle temperature T_R/T_0 (K)	Nozzle diameter d (μm)	Stagnation pressure p_0 (bar)	Concentration H_2O in Ar (%)	$\bar{n}$
1	H_2O	400/428	90	2.4	100	160
2	H_2O	420/428	90	4.2	100	435
3	H_2O/He	313/318	55	3.5	2.7	
4	H_2O/He	313/318	55	7.5	1.3	
5	H_2O/Ar	317/315	35	8.2	1.1	70 (Ar_n)
6	H_2O/Ar	317/315	35	11.0	0.81	110 (Ar_n)
7	H_2O/Ar	315/318	55	4.8	1.6	40 (Ar_n)

FIG. 1. Example of electron ionization mass spectra of mixed argon-water clusters. Experimental data in logarithmic scale (top) and integrated intensities for selected peaks (bottom). The expansion conditions correspond to no. 7 in Table I.

with very little mixed species and almost no pure Ar clusters observed.[33,34] In Sec. III, we demonstrate that also in the case of Ar/H_2O mixed expansions the generated cluster sizes and compositions can be quite different from what could be expected based on the above semiempirical formulas.

III. RESULTS AND DISCUSSION

In Subsections III A and III B, we address two interrelated questions: what is the structure of the mixed clusters and what are the dynamical processes following the ionization of mixed water-argon systems?

A. Neutral cluster structure

The structure of the neutral clusters can be revealed from the electron ionization measurements, using the information on the appearance energies of different ionic fragments. Before we do this, we shall briefly inspect the ionic fragments formed upon the 70 eV electron ionization of water clusters embedded in argon. Figure 1 shows the spectrum corresponding to conditions no. 7 in Table I. The bottom panel shows selected ion series from the top spectrum (integrated intensities; note the logarithmic and linear scales of the top and bottom spectra, respectively). The spectrum is dominated by Ar_n^+ series followed by the protonated water cluster ions $(H_2O)_nH^+$. These are the typical products of the electron impact on argon and water clusters, respectively. The $(H_2O)_nH^+$ ions are produced by reaction (1) followed by evaporation of relatively weakly bound OH radical and Ar atoms.

However, the present spectrum exhibits additional features in comparison with the pure Ar_n and $(H_2O)_n$ cluster ionization spectra. Namely, the mixed species $Ar_n(H_2O)_m^+$ and nonprotonated water cluster ions $(H_2O)_n^+$ are observed. The $(H_2O)_n^+$ ions are most likely formed again in reaction (1), however, the OH radical does not leave the cluster in this case[10–12] and the excess energy is carried away by the argon evaporation. These non-protonated water radical cations

in our spectra are present at significantly smaller abundances than in the excitonic transfer ionization spectra observed upon the argon photoexcitation.[18] Similarly, the $(H_2O)_n^+$ clusters were observed in helium droplets after electron ionization[16,17] in abundances of up to 10% of the protonated cluster ion signals. These abundances are comparable to our present results.

Even though the pure protonated $(H_2O)_nH^+$ ions are significantly more populated than $(H_2O)_n^+$, it is interesting to note that for the fragments with the Ar atoms still attached this is reversed; i.e., the $Ar_m(H_2O)_n^+$ ions are more populated than $Ar_m(H_2O)_nH^+$ (see Fig. 1; it should be noted that these mixed species are populated significantly only up to $n = 2$). Similar behaviour was observed previously in a photoionization study.[35] It is consistent with the assumption that the argon atoms are evaporated first and the OH radical leaves the cluster only if enough energy is still available after the evaporation of all argon atoms.

The nature of the mixed argon-water clusters can be revealed by the energy dependent yields of the particular fragments. Exploiting the different expansion conditions, we can demonstrate the solvent effects of the argon on the ionization of water upon gradually increasing the solvation, see Fig. 2. The figure shows the electron energy dependent ion yields of $(H_2O)_4H^+$ ions formed upon the ionization from different precursor clusters. The black curve corresponds to the pure water clusters. It shows monotonic increase in the whole energy range above the threshold of ≈12 eV. The blue curve corresponds to clusters formed in argon/water mixture expansion (conditions no. 5 in Table I). The shape changes noticeably, however, the threshold remains at ≈12 eV. This value indicates that water is still ionized directly, i.e., the water molecules are exposed to the incoming electrons. Diluting the expansion mixture further with Ar and arriving to the conditions no. 7 in Table I yields the red curve in Fig. 2. Here, the shape is markedly different from the curve measured with the pure water clusters exhibiting a two step structure typical for
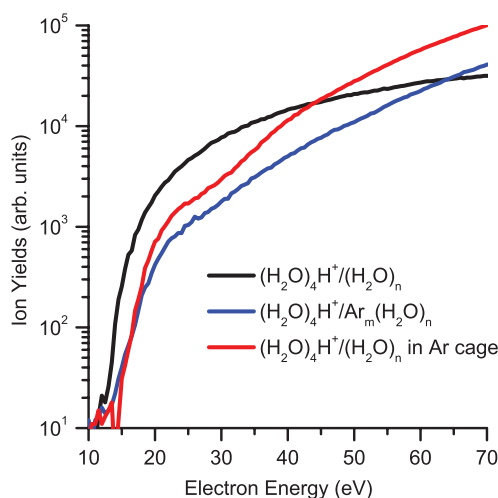

FIG. 2. Electron energy dependent ion yields for $(H_2O)_4H^+$ cluster ion formed in ionization of different types of precursor clusters: $(H_2O)_n$ clusters generated in pure water expansion (black line); $(H_2O)_n$ clusters generated in Ar-water expansion conditions no. 5 in Table I (blue line); Ar-coated $Ar_M(H_2O)_n$ clusters corresponding to conditions no. 7 in Table I (red line). See Fig. 4 for the detailed scans of the region between 11 eV and 19 eV.
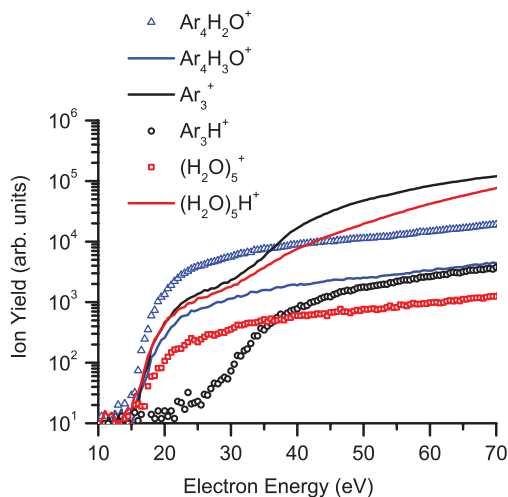
FIG. 3. Energy dependent ion yields for selected cluster ions formed in ionization of water clusters caged in Ar solvent.
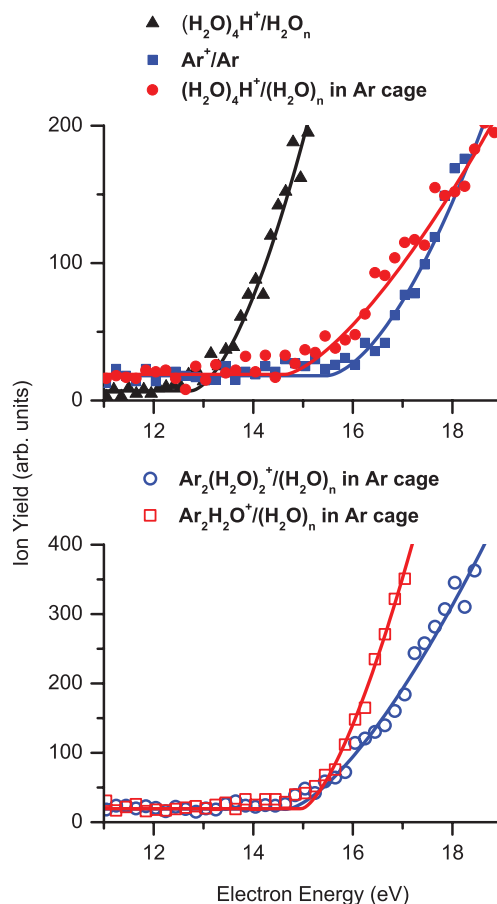

FIG. 4. Energy dependent ion yields near threshold for selected ions (scatter) and appropriate fits (lines) used to estimate the appearance potentials.

pure Ar clusters (see also Fig. 3). More importantly, the first threshold energy is now shifted to ≈15 eV which corresponds to the argon ionization in the cluster. Both the shape and especially the threshold indicate that the observed $(H_2O)_4H^+$ ion is generated in a process which starts with argon ionization. These processes will be discussed in more details in Sec. III B. It should be mentioned that the structure observed on the yield curves below 15 eV is within the noise limit and cannot be attributed to the resonance processes observed in the VUV experiments[18] (see also Fig. 4 for detailed energy scan of the region below 19 eV).

Fig. 3 shows the ionization yields of selected fragments produced after the ionization of clusters generated under expansion conditions no. 7 in Table I. To facilitate the comparison, we have chosen ion fragments of roughly comparable intensities (on the logarithmic scale). The other ions of the same type manifest similar energy dependencies. The appearance potentials of the particular ions were estimated by fits exemplified in Fig. 4. The values which were averaged from fits for several ions of the same type are listed in Table II. All the observed ions in the mixed clusters are produced at energies around 15 eV. This is significantly higher than the ionization potential of water (≈12.6 eV for bare molecule which is further lowered by more than 1 eV upon complexation[4]). The isolated Ar atom ionization potential is ≈15.7 eV, but the shift of the ionization threshold for Ar in clusters towards lower energies is not surprising.[36,37] Thus, the observed thresholds of ≈15 eV demonstrate that the ionization process for all the observed fragments apparently starts with the ionization of argon atom followed by an intracluster reactions (charge transfer) between the ionized argon atom and water units. The thresholds clearly indicate that the water clusters are fully coated by argon atoms under these conditions. It ought to be mentioned that Ar-coated small water clusters have also been suggested in some slit expansions based on shifts of infrared spectra.[38,39]

The fact that the clusters generated under the expansion conditions no. 7 are completely covered with argon layer is an interesting result contradicting the estimates based on

the semiempirical rules outlined in Sec. II. The mean cluster size of the Ar_n clusters generated in pure Ar expansion under conditions no. 7 is only $\bar{n} \approx 40$. The embedded water clusters must be significantly larger since ionized fragments with more than 100 water molecules can be observed in the spectra. However, 40 argon atoms can cover only about 10

TABLE II. Appearance energies (AE) for selected groups of ions. Average values obtained from n ranging between 2 and 8; m ranging between 13 and 15 for singly charged; and n between 41 and 47 (even) for doubly charged ions. The regions were selected to reduce possible overlaps with neighbouring mass peaks.

Neutral clusters	Ion	AE (eV)
Pure H₂O	$(H_2O)_nH^+$	12 ± 0.4
	$(H_2O)_nH_2^{2+}$	31.5 ± 2.0
Mixed H₂O–Ar	$(H_2O)_nH^+$	14.9 ± 0.4
	$H_2O_n^+$	14.8 ± 0.4
	Ar_n^+	15.2 ± 0.4
	$Ar_nH_2O^+$	14.9 ± 0.2
	$Ar_nH_3O^+$	14.9 ± 0.2
	$Ar_n(H_2O)_2^+$	14.7 ± 0.2
	$Ar_n(H_2O)_2H^+$	15.1 ± 0.2
	Ar_nH^+	28 ± 2
	$(H_2O)_mOH^+$	28 ± 2
	$(H_2O)_n^{2+}$	34.2 ± 2.0
	$(H_2O)_nH_2^{2+}$	34.4 ± 2.0

water molecules. Besides, the argon atoms are evaporating by the energy released upon coagulation of water into the clusters. Therefore, the present cluster structure of fully Ar-coated water clusters cannot be justified assuming that prevailingly argon clusters in expansions of Ar with only a few percent of water, and water adds and coagulates in the Ar clusters. Apparently, the clustering processes are more complex.

This conclusion is further supported by contrasting the source conditions no. 5 and 6 with those in no. 7. The former conditions would correspond to larger Ar_n clusters in pure Ar-expansions (Table I). Yet, they lead to smaller mixed clusters as revealed by the measured mass spectra extending to smaller fragments. In addition, the clusters generated under the conditions no. 5 and 6 have not been fully covered by argon which was revealed by the threshold measurements. Thus, the widely used Hagena's formulas[28–32] (2) and (3) cannot be applied for the mixed expansions without their further exploration and characterization.

B. Dynamical processes following the ionization

As we have discussed in the Introduction, the ejection of the HOMO electron triggers the proton transfer process in pure water clusters and the weakly bound OH radical fragments leave the cluster. For Ar-coated clusters, the argon cage serves as a bath into which the excess energy dissipates. This leads to an increase of the abundance of the nominally non-protonated clusters.

One of the motivations for the present study has been the recent observation of a strongly resonant process around 12 eV in the ionization of similar clusters with a tunable VUV radiation.[18] It has been argued that these ions are formed by an excitonic transfer according to a scheme: $(H_2O)_n Ar_m + h\nu \rightarrow (H_2O)_n Ar_m^* \rightarrow (H_2O)_n^+ Ar_m$. However, there is no evidence of such process in our electron ionization measurements. The lack of any significant ionic signal below 15 eV indicates that the excitonic energy transfer between argon and water is significantly less efficient than the ion-molecule reaction between the ionized Ar^+ and water. We can make a simple quantitative estimate: the cross section for the electron excitation of argon atom is $\sim 10^{-18}$ cm^2,[40] while the cross section for the ionization is $\sim 10^{-16}$ cm^2.[41] Since the intensities in our mass spectra span ~ 4 orders of magnitude, we would still be able to observe the excitonic ionization even if the efficiency of the excitonic transfer were as low as 1%. It is worth noting that also a previous detailed electron ionization study of mixed Ar–O$_2$ clusters did not reveal any evidence for the excitonic transfer at low energies.[42]

Several reasons can be discussed for the seemingly different results of the photon and electron ionization in Ar-covered clusters: First, we can assume that the excitonic transfer is only efficient if argon atoms are excited in the vicinity of water molecules. If the water cluster is coated with several argon layers, the Ar atoms in the bottom layer would have to be excited. Since the electron will not be able to penetrate into the large clusters, only the surface excitons will be formed which probably lead only to argon evaporation. On the other hand, the photons can excite the internal argon atoms in these clusters leading to the exciton transfer to water.

The second reason can be different sensitivity to the exciton transfer process in the photon and electron ionization. The photon fluxes in the synchrotron experiments are several orders of magnitude higher than the electron fluxes achievable by conventional electron sources. Therefore, the high number of the exciting photons and selectivity of the resonant Ar excitation process can lead to the observation of the excitonic transfer production of $(H_2O)_n^+$ clusters in the synchrotron experiments. However, the effectiveness of the resonant process in absolute numbers will be rather low in comparison to the non-resonant direct ionization, therefore, it is overwhelmed by the non-resonant processes in the electron ionization.

The third possibility to explain the differences can be the existence of competing channels found exclusively in electron ionization. Argon atoms are known to form core excited temporary negative ions upon electron irradiation at energies 11.6 eV which can be coupled to negatively charged and dissociative states in mixed clusters.[43] In solid phase, these couplings were also demonstrated for Ar–H$_2$O system.[44] A similar mechanism in our clusters would lead to an alternative decay mechanism for the exciton which would yield products other than the observed positive ions.

Although we have not observed the excitonic transfer at low electron energies, the ion yield curves indicate that such process can occur at higher energies. The Ar_n^+ ion yield dependencies (exemplified by Ar_3^+ in Fig. 3) exhibit a second strong increase around 25–30 eV while there is no secondary threshold for $(H_2O)_n H^+$ ion yield from pure $(H_2O)_n$ clusters (exemplified by $(H_2O)_4 H^+$ in Fig. 2). The signal enhancement at higher energies can be discussed in terms of various mechanisms: (1) double ionization of an Ar atom; (2) subsequent ionization of two argon atoms within one cluster; (3) ICD process leading to the double ionization. However, none of the mechanisms is consistent with the observed threshold. A plausible explanation is the ionization and excitation leading to the metastable Ar_n^{+*} ions proposed and explored in detail previously for Ar–O$_2$ system.[42] The ion-exciton pairs can be formed upon the ionization of the 3s electron in argon followed by an internal conversion process.[45] The decay of these excited Ar_n^{+*} clusters yields the smaller ionized fragments. These excited Ar_n^{+*} ions are formed at about 25–30 eV where the electron energy is sufficient to ionize and excite the Ar atoms in the cluster. In the mixed clusters, the exciton transfer can lead to the ionization of the partner molecule. In our Ar–H$_2$O system, the exciton transfer opens new reaction channels as demonstrated by the ions formed exclusively above ≈ 28 eV: $Ar_n H^+$ ions and $(H_2O)_n OH^+$ (see Fig. 3 and Table II).

Additionally, in Fig. 3 we see an increase in the signal of the protonated $(H_2O)_n H^+$ ions in the same energy region above ≈ 28 eV. Below this energy the $(H_2O)_n H^+$ ions are generated by argon ionization followed by the charge transfer process and reaction (1); above also the excitonic transfer contributes. Therefore, these ions can be formed by these two distinct processes. The mixed cluster ions $Ar_m(H_2O)_n H^+$ and $Ar_m(H_2O)_n^+$ as well as pure water cluster ions $(H_2O)_n^+$ do not exhibit the second threshold, i.e., they are not produced by the high energy excitonic transfer channel.
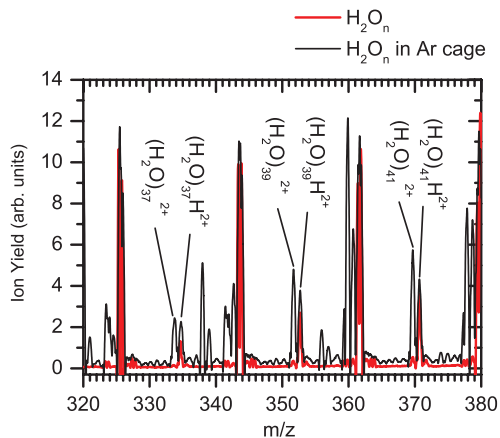
FIG. 5. Mass spectra of large pure water clusters (conditions no. 2, Table I) and Ar caged water clusters (conditions no. 7, Table I) at electron incident energy 80 eV. Extracted region showing the uprise of doubly charged ions.

We have also observed doubly charged ions in the spectra, see Fig. 5. There are pure doubly charged clusters $(H_2O)_n^{2+}$ and doubly protonated $(H_2O)_nH_2^{2+}$ ions generated from Ar coated clusters for $n \geq 36$. This size seems to be the smallest droplet which is able to support two positive charges. These doubly charged ions were observed previously from clusters also generated in Ar expansions.[46] However, in the pure water clusters only the doubly protonated ions $(H_2O)_nH_2^{2+}$ are formed, i.e., two hydroxyl radicals leave the clusters. This underlines the important role of Ar solvent which can stabilize the doubly ionized $(H_2O)_n^{2+}$ fragments. These ions are observed at energies above $\approx 34.2 \pm 2.0$ eV (see Fig. 6 and Table II). A precise determination of the threshold is not possible with the present resolution and low signal intensities, yet it is clearly above the ionization and excitation transfer process discussed above (≈ 28 eV), and below the double ionization limit of water (≈ 38 eV). Also the threshold for double protonated $(H_2O)_nH_2^{2+}$ ions from the pure water clusters at $\approx 31.5 \pm 2.0$ eV is somewhat lower than the threshold at $\approx 34.4 \pm 2.0$ eV from Ar caged clusters.
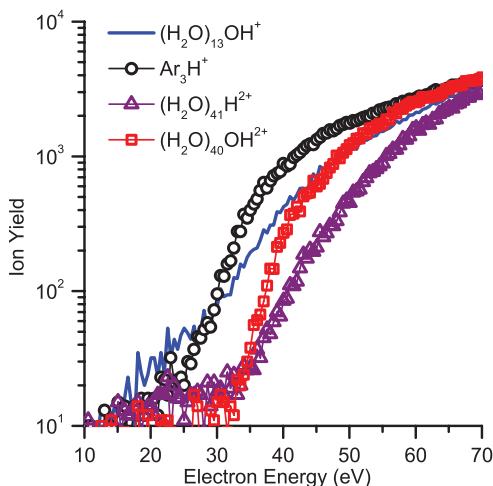

FIG. 6. Energy dependent ion yields for selected cluster ions formed in ionization of water clusters caged in Ar solvent.

From the above energy thresholds for pure and argon coated water clusters, we can make some tentative conclusions about the mechanism of the doubly charged ion formation. The simplest explanation is sequential two-step ionization (as observed, e.g., for Ar[47]). This process in water clusters should be observed at electron energies well below ~ 25 eV, which is clearly not the case. In the case of pure water clusters, the threshold at 31.5 eV correlates well with the double ionization and subsequent dissociation of a single water molecule in the gas phase, which results into $H^+ + OH^+$ products.[48] Alternatively, the $(H_2O)_nH_2^{2+}$ type ions can be formed within the ICD process. Here, the two positive charges are formed in two directly neighboring molecular units. The ICD channel was shown to be open upon the ejection of the $2a_1$ electron in small water clusters above 30 eV.[21, 22] When the clusters are Ar-coated, the process starts with Ar ionization. The sequential ionization of two Ar atoms within the cluster should occur at somewhat lower energies, slightly below ~ 30 eV. The present threshold above ≈ 34 eV is rather consistent with the ICD process. The ICD process was identified at around 35 eV for argon dimer[45] and this energy should be lowered by the electronic polarization in larger clusters.

IV. CONCLUSIONS

We have investigated the electron ionization of mixed water–Ar clusters. The measurements of electron energy dependent ion yields have revealed that under certain expansion conditions water clusters fully covered with the argon solvation shell are generated. Thus, we have demonstrated that the electron ionization mass spectrometry can serve as a tool to determine the cluster composition and structure in some special cases. We also point out the limited applicability of the widely used semiempirical formulas for mean cluster size determination.

The present study has also demonstrated important solvent effects on the water cluster ionization. First, the Ar solvent layer shields the embedded $(H_2O)_n$ clusters. Therefore, the ionization starts only at 15 eV corresponding to the electron energy threshold for Ar-ionization in the cluster.

Second, the argon can act as a mediator of more complex reactions in the clusters. The direct charge transfer process between Ar^+ and water results in the water fragmentation expected for reaction (1). However, at higher electron energies above ~ 28 eV an excitonic transfer process opens between Ar_n^{+*} and water, resulting into the dissociative ionization of water to either OH^+ or H^+. This pathway leads further to either $(H_2O)_nOH^+$ fragments, or to Ar_nH^+ and $(H_2O)_nH^+$ ions, respectively. Although this excitonic transfer reaction from the ion excited state Ar_n^{+*} contributes strongly above ~ 28 eV, the excitonic transfer from the neutral Ar* state at lower energies has not been detected in the present experiments despite the fact that a strong resonance effect was observed in the photoionization experiment at 11.9 eV.[18]

The third effect of argon on the cluster ionization is its stabilization via efficient energy removal from the cluster by Ar evaporation. This is the main stabilization mechanism for the unprotonated water clusters $(H_2O)_n^+$, formed upon electron ionization of argon and subsequent charge transfer. The

effectiveness of the energy flow is also demonstrated by the observation of doubly charged ions. The doubly charged clusters contain two singly charge units and the argon evaporation significantly helps to stabilize such systems. The observation of the non-protonated doubly charged clusters $(H_2O)_n^{2+}$ in the argon coated cluster is yet another manifestation of the argon stabilization effect as the argon atoms take away the energy released during the proton transfer processes following the ionization.

The threshold energies for a formation of doubly charged clusters is different for bare and argon-coated clusters. These thresholds are in both cases energetically consistent with the intermolecular Coulomb decay process. The present experiment thus provides a (tentative) evidence of the ICD process taking place in water clusters above 30 eV.

The study shows that even so extensively studied interaction as electron ionization of water is still not fully understood especially in a solvent even as simple as the rare gas argon.

[1] B. C. Garrett, D. A. Dixon, D. M. Camaioni, D. M. Chipman, M. A. Johnson, C. D. Jonah, G. A. Kimmel, J. H. Miller, T. N. Rescigno, P. J. Rossky, S. S. Xantheas, S. D. Colson, A. H. Laufer, D. Ray, P. F. Barbara, D. M. Bartels, K. H. Becker, K. H. Bowen, S. E. Bradforth, I. Carmichael, J. V. Coe, L. R. Corrales, J. P. Cowin, M. Dupuis, K. B. Eisenthal, J. A. Franz, M. S. Gutowski, K. D. Jordan, B. D. Kay, J. A. LaVerne, S. V. Lymar, T. E. Madey, C. W. McCurdy, D. Meisel, S. Mukamel, A. R. Nilsson, T. M. Orlando, N. G. Petrik, S. M. Pimblott, J. R. Rustad, G. K. Schenter, S. J. Singer, A. Tokmakoff, L.-S. Wang, and T. S. Zwier, Chem. Rev. **105**, 355 (2005).

[2] A. Mozumder and Y. Hatano, *Charged Particles and Photon Interactions with Matter: Chemical, Physicochemical and Biological Consequences with Applications* (CRC Press, 2003).

[3] L. Belau, K. R. Wilson, S. R. Leone, and M. Ahmed, J. Phys. Chem. A **111**, 10075 (2007).

[4] S. Barth, M. Ončák, V. Ulrich, M. Mucke, T. Lischke, P. Slavíček, and U. Hergenhahn, J. Phys. Chem. A **113**, 13519 (2009).

[5] O. Svoboda, M. Ončák, and P. Slavíček, J. Chem. Phys. **135**, 154302 (2011).

[6] B. Winter, R. Weber, W. Widdra, M. Dittmar, M. Faubel, and I. V. Hertel, J. Phys. Chem. A **108**, 2625 (2004).

[7] O. Maršálek, C. G. Elles, P. A. Pieniazek, E. Pluhařová, J. VandeVondele, S. E. Bradforth, and P. Jungwirth, J. Chem. Phys. **135**, 224510 (2011).

[8] O. Svoboda, D. Hollas, M. Ončák, and P. Slavíček, Phys. Chem. Chem. Phys. **15**, 11531 (2013).

[9] K. Hansen, P. U. Andersson, and E. Uggerud, J. Chem. Phys. **131**, 124303 (2009).

[10] G. H. Gardenier, M. A. Johnson, and A. B. McCoy, J. Phys. Chem. A **113**, 4772 (2009).

[11] K. Mizuse and A. Fujii, J. Phys. Chem. A **117**, 929 (2013).

[12] R. T. Jongma, Y. Huang, S. Shi, and A. M. Wodtke, J. Phys. Chem. A **102**, 8847 (1998).

[13] M. Ehbrecht, M. Stemmler, and F. Huisken, Int. J. Mass Spectrom. **123**, R1 (1993).

[14] G. Vaidyanathan, M. T. Coolbaugh, W. R. Peifer, and J. F. Garvey, J. Chem. Phys. **94**, 1850 (1991).

[15] G. Vaidyanathan, M. T. Coolbaugh, W. R. Peifer, and J. F. Garvey, J. Phys. Chem. **96**, 1589 (1992).

[16] S. Denifl, F. Zappa, I. Mähr, F. F. da Silva, A. Aleem, A. Mauracher, M. Probst, J. Urban, P. Mach, A. Bacher, O. Echt, T. D. Märk, and P. Scheier, Angew. Chem., Int. Ed. **121**, 9102 (2009).

[17] S. Denifl, F. Zappa, I. Mähr, A. Mauracher, M. Probst, J. Urban, P. Mach, A. Bacher, D. K. Bohme, O. Echt, T. D. Märk, and P. Scheier, J. Chem. Phys. **132**, 234307 (2010).

[18] A. Golan and M. Ahmed, J. Phys. Chem. Lett. **3**, 458 (2012).

[19] B. Kamke, W. Kamke, Z. Wang, E. Ruhl, and B. Brutschy, J. Chem. Phys. **86**, 2525 (1987).

[20] K. Ohno, H. Tanaka, Y. Yamakita, R. Maruyama, T. Horio, and F. Misaizu, J. Electron Spectrosc. Relat. Phenom. **112**, 115 (2000).

[21] M. Mucke, M. Braune, S. Barth, M. Forstel, T. Lischke, V. Ulrich, T. Arion, U. Becker, A. Bradshaw, and U. Hergenhahn, Nat. Phys. **6**, 143 (2010).

[22] T. Jahnke, H. Sann, T. Havermeier, K. Kreidi, C. Stuck, M. Meckel, M. Schoffler, N. Neumann, R. Wallauer, S. Voss, A. Czasch, O. Jagutzki, A. Malakzadeh, F. Afaneh, T. Weber, H. Schmidt-Bocking, and R. Dorner, Nat. Phys. **6**, 139 (2010).

[23] M. Fárník, *Molecular Dynamics in Free Clusters and Nanoparticles Studied in Molecular Beams* (ICT Prague Press, Institute of Chemical Technology Prague, 2011).

[24] J. Lengyel, A. Pysanenko, J. Kočišek, V. Poterya, C. Pradzynski, T. Zeuch, P. Slavíček, and M. Fárník, J. Phys. Chem. Lett. **3**, 3096 (2012).

[25] J. Kočišek, J. Lengyel, and M. Fárník, J. Chem. Phys. **138**, 124306 (2013).

[26] S. Kaesdorf, *Geräte für forschung und industrie, Munich*, 2011, http://www.kaesdorf.de/.

[27] A. R. Milosavljevic, J. Kočišek, P. Papp, D. Kubala, B. P. Marinkovic, P. Mach, J. Urban, and S. Matejčik, J. Chem. Phys. **132**, 104308 (2010).

[28] O. F. Hagena, Surf. Sci. **106**, 101 (1981).

[29] O. F. Hagena, Z. Phys. D **4**, 291 (1987).

[30] O. F. Hagena, Rev. Sci. Instrum. **63**, 2374 (1992).

[31] U. Buck and R. Krohne, J. Chem. Phys. **105**, 5408 (1996).

[32] C. Bobbert, S. Schütte, C. Steinbach, and U. Buck, Eur. Phys. J. D **19**, 183 (2002).

[33] R. Baumfalk, U. Buck, C. Frischkorn, S. R. Gandhi, and C. Lauenstein, Chem. Phys. Lett. **269**, 321 (1997).

[34] R. Baumfalk, U. Buck, C. Frischkorn, S. R. Gandhi, and C. Lauenstein, Ber. Bunsenges. Phys. Chem. **101**, 606 (1997).

[35] H. Shinohara, N. Nishi, and N. Washida, J. Chem. Phys. **84**, 5561 (1986).

[36] P. Svrčková, A. Vítek, F. Karlický, I. Paidarová, and R. Kalus, J. Chem. Phys. **134**, 224310 (2011).

[37] O. Echt, T. Fiegele, M. Rümmele, M. Probst, S. Matt-Leubner, J. Urban, P. Mach, J. Leszczynski, P. Scheier, and T. D. Märk, J. Chem. Phys. **123**, 084313 (2005).

[38] D. Nesbitt, T. Häber, and M. A. Suhm, Discuss. Faraday Soc. **118**, 305 (2001).

[39] A. Moudens, R. Georges, M. Goubet, J. Makarewicz, S. E. Lokshtanov, and A. A. Vigasin, J. Phys. Chem. **131**, 204312 (2009).

[40] S. J. Buckman, P. Hammond, G. C. King, and F. H. Read, J. Phys. B **16**, 4219 (1983).

[41] R. Rejoub, B. G. Lindsay, and R. F. Stebbings, Phys. Rev. A **65**, 042713 (2002).

[42] M. Foltin, T. Rauth, V. Grill, P. Lukáč, and T. D. Märk, Int. J. Mass Spectrom. Ion Process. **134**, 23 (1994).

[43] T. Jaffke, R. Hashemi, L. Christophorou, and E. Illenberger, Z. Phys. D **25**, 77 (1992).

[44] P. Rowntree, H. Sambe, L. Parenteau, and L. Sanche, Phys. Rev. B **47**, 4537 (1993).

[45] P. Lablanquie, T. Aoto, Y. Hikosaka, Y. Morioka, F. Penent, and K. Ito, J. Chem. Phys. **127**, 154323 (2007).

[46] N. G. Gotts, P. G. Lethbridge, and A. J. Stace, J. Chem. Phys. **96**, 408 (1992).

[47] P. Scheier and T. D. Märk, J. Chem. Phys. **86**, 3056 (1987).

[48] S. Truong, A. Yencha, A. Juarez, S. Cavanagh, P. Bolognesi, and G. King, Chem. Phys. Lett. **474**, 41 (2009).